Journal of Marine Science and Engineering

MDPI

Article

A 3D Innovative Approach Supporting the Description of Boring Sponges of the Precious Red Coral *Corallium rubrum*

Torcuato Pulido Mantas [1,*], Giorgio Bavestrello [2], Marco Bertolino [2,†], Carlo Cerrano [1], Daniela Pica [3], Camilla Roveta [1] and Barbara Calcinai [1,†]

[1] Dipartimento di Scienze della Vita e dell'Ambiente (DiSVA), Università Politecnica delle Marche, Via Brecce Bianche, 60131 Ancona, Italy; c.cerrano@staff.univpm.it (C.C.); c.roveta@pm.univpm.it (C.R.); b.calcinai@univpm.it (B.C.)

[2] Dipartimento di Scienze della Terra dell'Ambiente e della Vita (DISTAV) Corso Europa 26, 16132 Genova, Italy; giorgio.bavestrello@unige.it (G.B.); marco.bertolino@unige.it (M.B.)

[3] Department of Integrative Marine Ecology, Stazione Zoologica Anton Dohrn, Calabria Marine Centre, C. Torre Spaccata, 87071 Amendolara, Italy; daniela.pica@szn.it

* Correspondence: t.pulido@pm.univpm.it

† These authors have contributed equally to this work.

Abstract: The carbonatic scleraxis of *Corallium rubrum* (L.), commonly known as red coral, is often found infested by excavating sponges. These boring organisms produce galleries inside the compact axis of the coral in a variety of shapes compromising the integrity of the skeleton and reducing its commercial value. Three sponge species, already known to bore into *Corallium rubrum*, have been identified in colonies collected from Cape Verde Archipelago—*Alectona millari* (Carter, 1879); *Dotona pulchella mediterranea* (Rosell and Uriz, 2002); and *Thoosa armata* (Topsent, 1888)—together with a new species belonging to the genus *Alectona* and here described. SEM analysis provided evidence of the microerosion patterns of these species, confirming the presence of radial scars overlapped with the concentric ones, in *T. armata*. For the first time, microcomputed tomography was employed to obtain three-dimensional reconstructions of sponge excavations inside the red coral scleraxis and to estimate the eroded volume.

Keywords: bioerosion; Porifera; *Alectona*; *Thoosa*; *Dotona*; new species; micro-CT; Cape Verde

Citation: Mantas, T.P.; Bavestrello, G.; Bertolino, M.; Cerrano, C.; Pica, D.; Roveta, C.; Calcinai, B. A 3D Innovative Approach Supporting the Description of Boring Sponges of the Precious Red Coral *Corallium rubrum*. *J. Mar. Sci. Eng.* **2022**, *10*, 868. https://doi.org/10.3390/jmse10070868

Academic Editor: Azizur Rahman

Received: 3 May 2022
Accepted: 21 June 2022
Published: 24 June 2022

1. Introduction

Boring sponges are among the main actors shaping coral reefs and calcareous substrates in general [1]. Impacts of sponge erosion are widely studied in tropical areas, while few data are available for temperate and mesophotic corals. In particular, regarding octocorals, the scleraxis of the precious corals belonging to the family Coralliidae from the Mediterranean Sea and the Pacific Ocean is frequently damaged by excavating sponges which produce galleries of various sizes and shapes [2–4], compromising the integrity of the skeleton, likely limiting colony stability and reducing its commercial value [5,6]. In particular, the red coral skeleton is the preferential substrate for several species belonging to the genera *Thoosa, Alectona*, and *Dotona* [4].

The genus *Alectona* is characterised by the presence of diactinal (sometimes polyactinal) spicules, fusiform amphiasters, and by the lack of tylostyles [7]. Its bioerosive activity produces erosion marks, the so-called pitting pattern, characterised by concentric grooves overlapped by radiating scars [8,9]. Species of *Alectona*, known so far as excavating into red coral, are 6 out of 11 [4,10]: *A. millari* (Carter, 1879); *A. sorrentini* (Bavestrello, Calcinai, Cerrano, and Sarà, 1998); *A. triradiata* (Lévi and Lévi, 1983); *A. wallichii* (Carter, 1874); *A. verticillata* (Johnson, 1899); and *A. sarai* (Calcinai, Cerrano, Iwasaki, and Bavestrello, 2008).

Dotona species are characterised by styles or strongyles as main spicules, and by spiny microstrongyles and diplasters as microscleres [7]. This genus includes two species, *D. pulchella* (Carter, 1880), which is known to excavate into the red coral [4], and *D. davidi* (Kirkpatrick, 1900), documented only inside the scleractinian coral *Echinopora* sp.

In the case of the genus *Thoosa,* tylostyles or oxeas may be present as megascleres (missing in some species), and amphiasters and oxyasters as typical microscleres. Out of 16 known species of *Thoosa* [10], *T. armata* (Topsent, 1888), *T. bulbosa* (Hancock, 1849), *T. midwayi* (Azzini et al. 2007), and *T. mollis* (Volz, 1939) have been recorded boring into the red coral from the Mediterranean Sea and the Indo-Pacific Ocean [4].

Until today, studies on boring sponges are mainly based on destructive methods to measure endolithic sponge biomass and consequently the volume of eroded substrate [11]. In recent years, microcomputed tomography (micro-CT) has begun to be used to analyse, describe, and quantify sponge erosion, avoiding the destruction of the material [11–13]. Erosion chambers are, in general, well-visualised with this technique but, depending on the resolution power of the CT scanner, fine details, such as pioneer filaments used by the sponge to go forward in the substrate, or erosion scars cannot be well-resolved [11].

In some colonies of red coral sampled at the Cape Verde Archipelago, we detected the presence of three already known excavating sponges together with a new species, here described. Coupled with the traditional taxonomic approaches, we propose the application of the micro-CT on the coral samples to observe the three-dimensional architecture of sponge erosion, obtaining a more complete and detailed morphological description of the chambers and the volume eroded inside the scleraxis.

2. Materials and Methods

Five samples of *Corallium rubrum* (Linnaeus, 1758) collected at Cape Verde, kindly supplied by the Museo Civico di Storia Naturale di Genova (Genoa, Italy), were analysed. The collection consists of old colonies stored in the Museum, and data about the exact sampling location(s), depth(s), or date(s) of the collection are not available.

The sponge spicule complement was analysed according to Rützler [14]. Spicule size range, mean and standard deviation (SD) were obtained from 15 measurements per spicule type. Spicules were also analysed with a scanning electron microscope (SEM); thus, spicule dissociations were transferred onto stubs and sputtered with gold. Erosion chambers and excavation scars were also studied using both SEM and optical microscopy. For SEM observation, fragments of *C. rubrum* were put on stubs and sputtered with gold. Pit dimensions (maximal diameter, n = 15) were measured on SEM images using ImageJ 1.37, avoiding pioneer areas of the erosion chambers. The SEM studies were carried out using a Philips XL 20 SEM.

Sponges' erosive patterns were assessed via micro-CT. The scanning of the red coral samples was performed with the Skyscan 1174 of the Centro di Ricerca e Servizio di Microscopia delle Nanostrutture (CISMiN) at the Università Politecnica delle Marche (Italy). The tomograph was equipped with an X-ray source (20–50 kV) and a flat panel detector with 1304×1024 pixels. Additionally, an aluminium filter was placed between the sample and the X-ray source to maximise the energy transmission through the sample. During scanning, the X-ray source was set at 50 kV and 800 μA, and the sample was rotated a total of 180° by 0.36° angular increments, acquiring an X-ray absorption radiograph at each rotation step. Raw data were preprocessed with cone-beam reconstruction software (Nrecon v.1.7.3.1., Skyscan), resulting in a series of axial cross-sections with a range of pixel sizes from 9.6 to 28.5 μm.

Postprocessing of the cross-sections was conducted using the AMIRA-Avizo software by Thermo Fisher Scientific. Firstly, a 3D-mode iterative median filter was applied to reduce image noise. Then, sponge cavities were segmented from the coral substrate by the following workflow: (1) the interactive thresholding module binarised the cross-sections, defining the coral skeleton as solid material; (2) the production of "digital casts"

from the empty cavities inside the coral were obtained applying ambient occlusion module over the binarised images allowed; (3) a second interactive thresholding module was implemented to calculate the eroded volumes; (4) lastly, species designation to the digital casts were validated by coupling spicules and pits observations.

All dimension metrics extracted from the three-dimensional reconstructions were obtained with the help of the axial cross-sections and the measurements module. When a single sponge species was present inside the sample, the volume eroded by the sponge was calculated; when it was not possible to assign the erosion traces at the level of the single species, the volume of sponge erosion was expressed as the total erosion volume referring to all of the sponges present in the sample. Three-dimensional models of the erosive patterns obtained from the five analysed samples are provided as Supplementary Material in File S1, and metrics from the eroded traces are presented in Table S1.

The type material of the new species, together with the entire collection, is deposited at the Museo Civico di Storia Naturale "G. Doria" of Genova (MSNG), Italy.

3. Results

3.1. Erosion Pattern and Excavated Volume

Four species of boring sponges—*Alectona millari, Alectona ricardi* sp. nov., *Thoosa armata*, and *Dotona pulchella mediterranea*—were detected in the five samples of *Corallium rubrum* and herein described (Figures 1–9). The coral samples presented different percentages of eroded volume. In the first sample (CT3, Figure 1), *D. pulchella mediterranea* and *A. millari* were detected, eroding 40.15% of the total volume of the sample. In the second sample (CTX, Figure 4), three species were identified: A branch of CTX was excavated by *D. pulchella mediterranea* and *A. ricardi* sp. nov. (Figure 4b–d) that, in the complex, were responsible for the erosion of 22.14% of the total volume, while the second branch included *D. pulchella mediterranea* and *A. millari* (Figure 1d–f) that eroded up to the 30.40% of the volume. The third and the fourth samples (CT5 and CT6, Figure 5) were exclusively bored by *T. armata*, eroding 20.08% and 13.48% of the samples' volume, respectively. Finally, the fifth sample (CT2, Figure 8) was exclusively excavated by *D. pulchella mediterranea*, which removed 7.79% of scleraxis.

3.2. Taxonomy

Order Tetractinellida Marshall, 1876
Suborder Thoosina Carballo, Bautista-Guerrero, Cárdenas, Cruz-Barraza, and Aguilar-Camacho, 2018
Family Thoosidae Cockerell, 1925
Genus *Alectona* Carter, 1879
Alectona millari Carter, 1879

Material

This sponge was present in a small red coral sample (CT3, Figure 1a) of 1.7 cm high and 0.8 cm in diameter, together with *D. pulchella mediterranea,* and in a second larger branched colony of *C. rubrum* (CTX, Figure 1d) of about 5.5 cm high and 2.5 cm in diameter at its base, where *D. pulchella mediterranea* and *A. ricardi* sp. nov. were also detected.

Taxonomic description

Spicules: Long acanthoxeas sometimes are shown as bent or curved, with blunt spines at the apex, scattered along the shaft (Figure 2a–d). Some spicules are only slightly spiny (Figure 2c), while others are bifurcated (Figure 2e). Measurements are 225 (245.5 ± 10.1) 260 × 15 (19.4 ± 2.5) 22.5 μm. Smooth oxeas sometimes have a central knob or are curved (Figure 2f,g). Measurements are 165 (198 ± 19) 225 × 12 (14.6 ± 2.2) 18 μm. Amphiasters are characterised by spiny knobs and are irregularly arranged (Figure 2h–k). Some are thinner and short with pointed extremities. Measurements are 20 (44 ± 14.4) 65 μm. Numerous armed larvae were detected inside the chambers (Figure 2l). A layer of discotriaenes covers the larva with sinuous, thin styles (450 (534.1 ± 93.8) 664 × 2.5–5 μm) radiating from

its centre (Figure 2l,m). The discotriaenes are flattened and triangular (Figure 2l,n,o); measurements of the diameter are 107.5 (125 ± 9.8) and 137.5 µm. The outer surface has, sometimes, a sort of triangular depression and is rough (Figure 2l,n), while the inner surface is convex and smooth, with a central, short rhabd (Figure 2o).

Erosion pattern: A. millari developed mainly in the central section of the coral axis, excavating large subspherical erosion chambers. In the first sample (CT3, Figure 1a) where *A. millari* was present along with *D. pulchella mediterranea* (Figure 1b; File S1), the only detected chamber was 5.19 × 11.13 mm wide (Figure 1c), while in the sample where *A. millari* shared the substrate with *D. pulchella mediterranea* and *A. ricardi* sp. nov., it was possible to recognise three chambers: a small one of 1.38 mm × 2.89 mm and two large irregular cavities 4.9–5.3 × 13–14 mm separated from each other by a short connecting duct of 2 mm in length (Figure 1e,f; File S1; Table S1). Only in one sample (CTX) was it possible to detect papillary channels of 0.13–1 mm in length, reaching the coral surface through papillae of 0.12 to 0.30 mm in diameter (Table S1).

The SEM analysis of the walls of the erosion chambers showed pits of 77.5 ± 10.8 µm decorated with concentric and radial lines (Figure 3a).

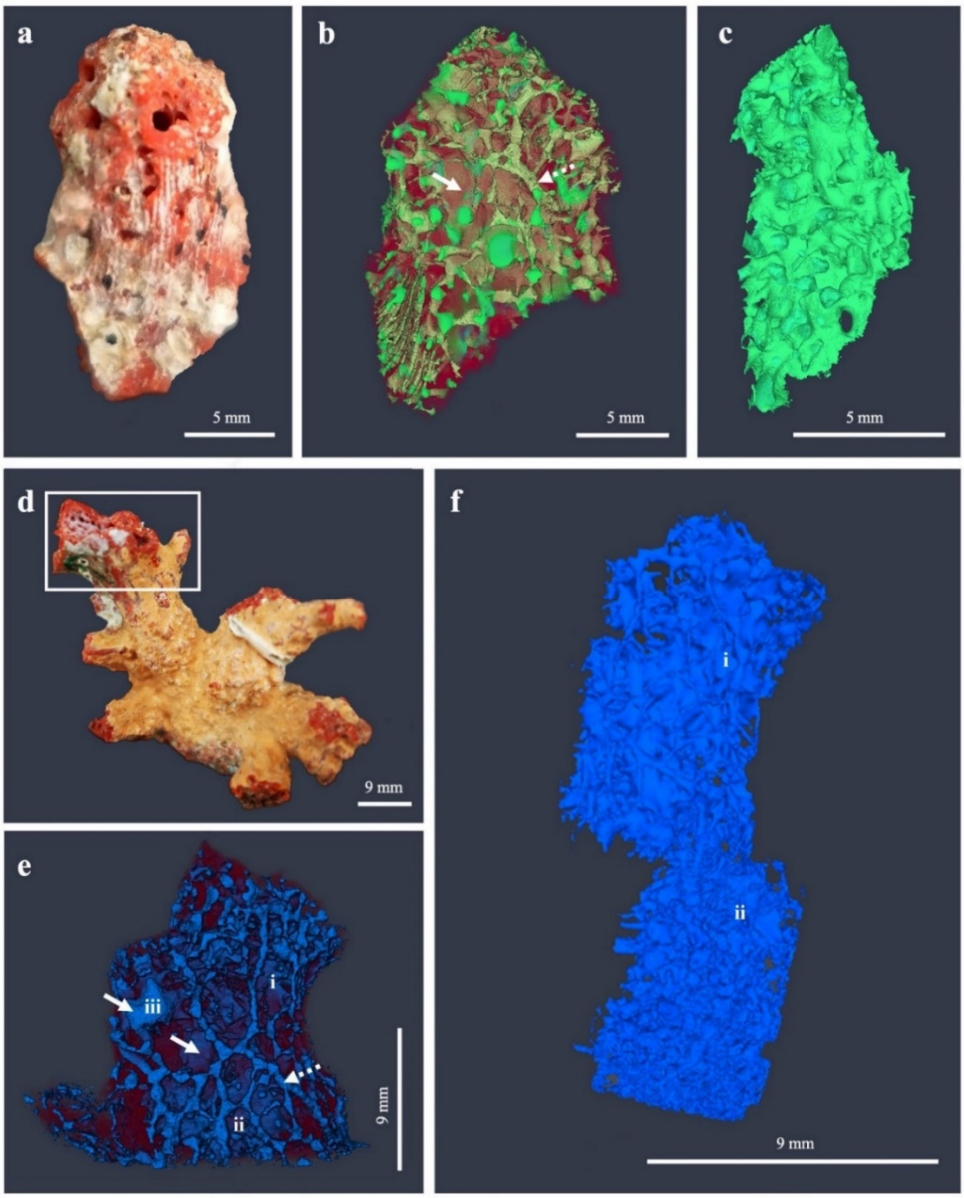

Figure 1. Three-dimensional visualisation of the red coral samples excavated by *Alectona millari*, from micro-CT reconstructions: (**a**) red coral sample CT3 showing the sponge papillae; (**b**) eroded

cavities are in green and coral in transparent red, the continuous arrow points to the chamber of *A. millari,* surrounded by the chambers of *Dotona pulchella mediterranea* (dotted arrow); (**c**) system of cavities of *A. millari* after a manual cleaning of most of *D. pulchella mediterranea* surrounding erosive activity; (**d**) red coral sample CTX; the area inside the rectangle is the location where the scanning efforts were focused; (**e**) digital cast showing the sponge eroded systems in blue and the coral skeleton in transparent red, the continuous arrows mark two of the chambers of *A. millari*, while the dotted arrow marks the chambers of *D. pulchella mediterranea*; (**f**) erosive activity of *A. millari* after a manual cleaning of *D. pulchella mediterranea* erosive cavities. Chambers i and ii correspond to the ones shown in (**e**).

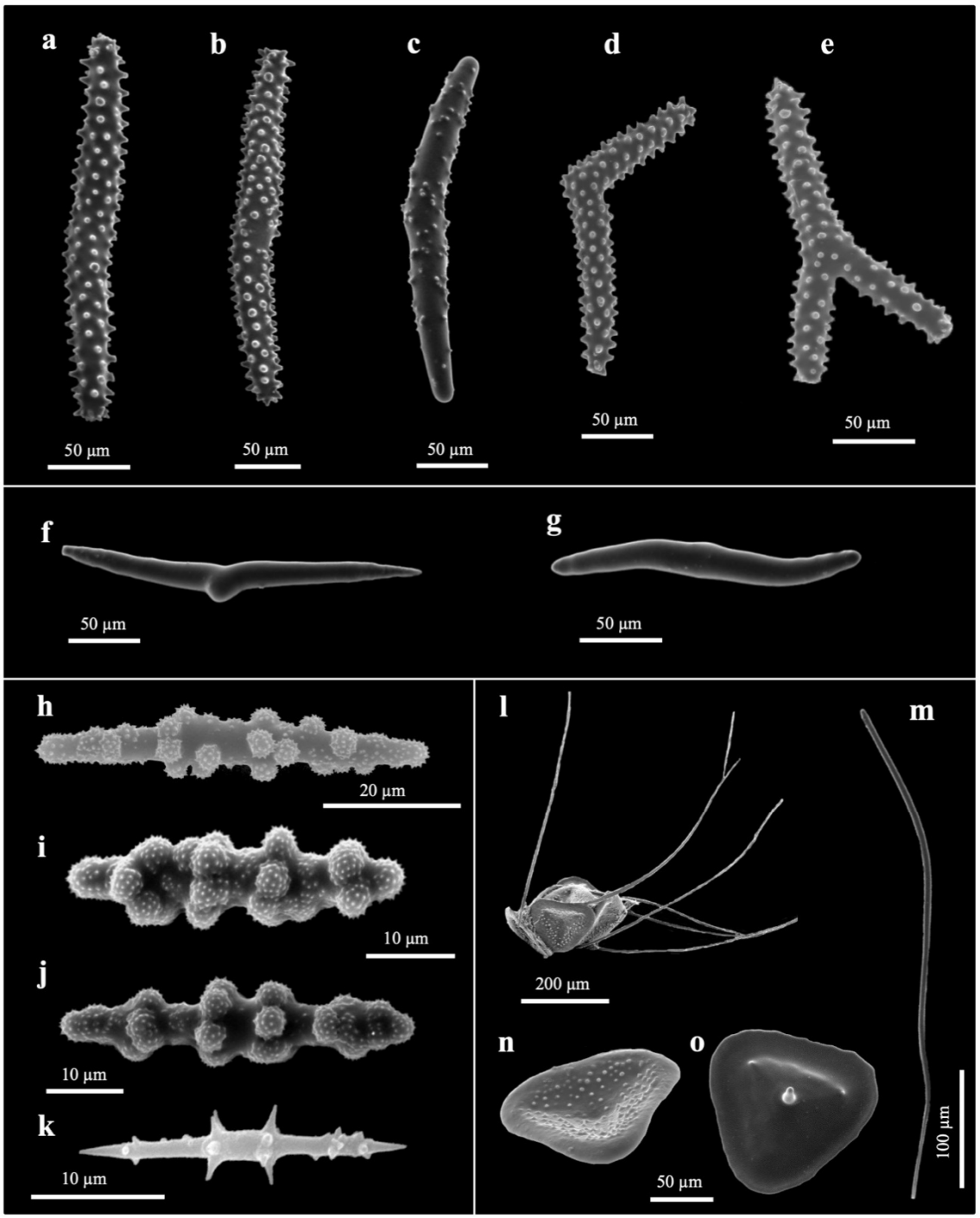

Figure 2. Spicule composition of *Alectona millari.* SEM images: (**a**–**d**) long acanthoxeas, with flattened spines scattered along the shaft; (**e**) acanthoxea showing a lateral ray, with a similar appearance to that of spined triactine; (**f**,**g**) curved, small, and smooth oxeas; (**h**–**k**) irregular spiny amphiasters; (**l**)

armed larva; (**m**) thin sinuous style from larva surface; (**n**,**o**) outer and inner faces of the discotriaenes covering the larvae, respectively.

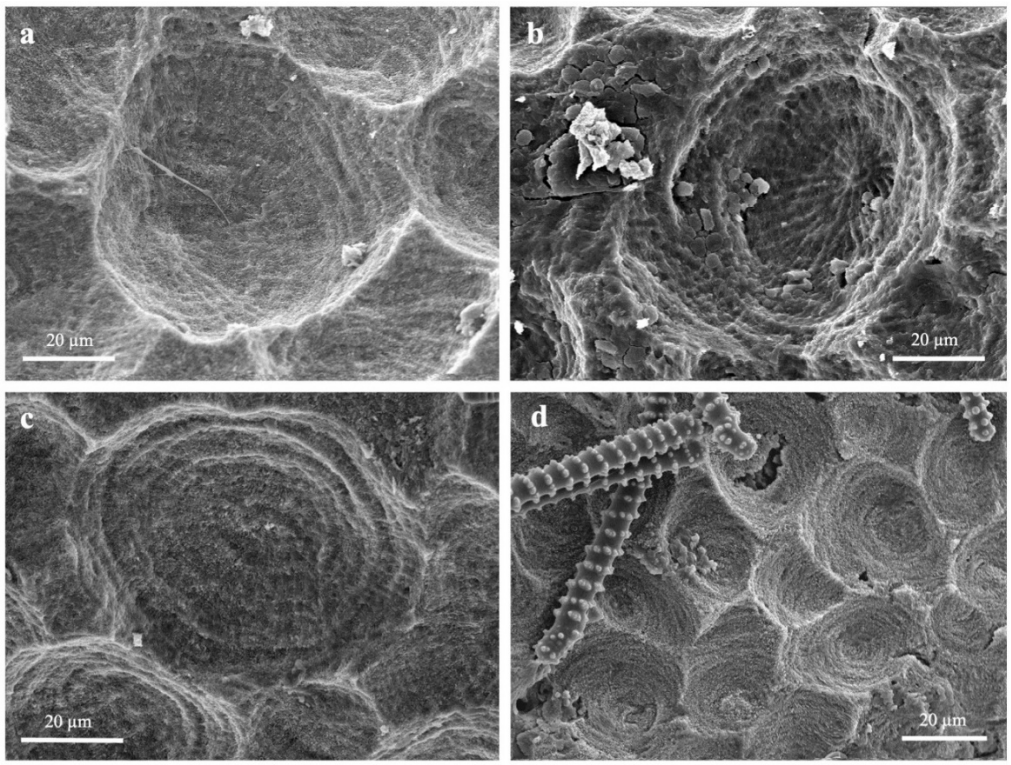

Figure 3. SEM images of sponge-generated bioerosion chambers, showing in the walls the characteristic pits of the different species recorded in the red coral samples: (**a**) *Alectona millari*; (**b**) *A. ricardi* sp. nov.; (**c**) *Thoosa armata*; (**d**) *Dotona pulchella mediterranea*. In c, the presence of radial scars superimposed on concentric lines was previously only reported by [15,16].

Remarks

This species has been described as boring into several kinds of substrates such as scleractinians, shells, rocks, and red coral, as reported in, for instance, [4,17]. The description of the *A. millari* cavities system obtained via micro-CT observations agreed with the literature [17], where the erosion pattern is described as a network of massive central chambers from which pioneer filaments extend. Among our samples, this is the species that presented a wider variation in terms of chamber morphology, possibly due to the co-occurrence with two other sponge species in the same colony (Figure 1b,e); in fact, it has been documented for other boring sponges that their characteristic erosive pattern may be strongly modified by the interactions with other bioeroders competing for the same substrate [13,18,19].

No description of ichnotaxa holding similar erosion patterns was found in the literature.

Alectona ricardi Calcinai and Bertolino sp. nov.

urn:lsid:zoobank.org:pub:5A5AAF18-5929-4938-A6B0-D86B570FCED0

Diagnosis

This species is characterised by spiny triactines and thin nodular amphiasters (Figure 5).

Material

Holotype: MSNG 62433.

Alectona ricardi sp. nov. occupied one of the ramifications of a *C. rubrum* colony of about 5.5 × 2.5 cm (CTX, Figure 4a), along with *A. millari* and *D. pulchella mediterranea* (Figure 4b). No data about sampling coordinates and depth are available.

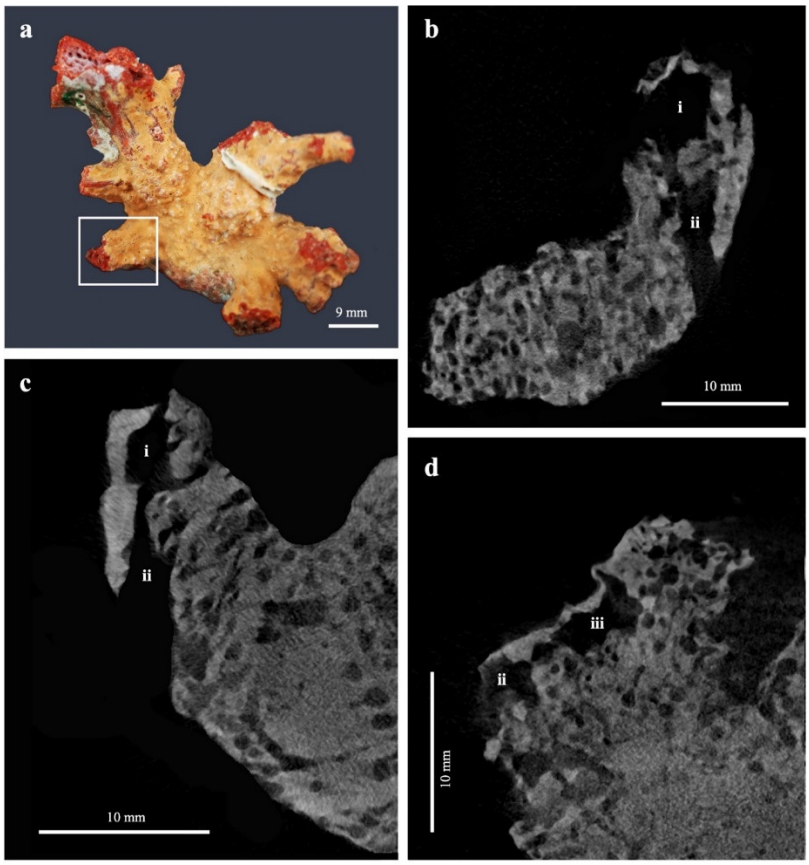

Figure 4. Red coral sample excavated by *Alectona ricardi* sp. nov. along with cross-sections from micro-CT scans: (**a**) red coral sample CTX; the marked area is the part of the sample where the new species was detected; (**b**) perpendicular (xz) cross-section showing two of the three cameras (i,ii) of *A. ricardi* sp. nov.; (**c**) perpendicular cross-section (xy) showing the same two cameras (i,ii) with a different perspective; (**d**) transversal cross-section (yz) showing the second and the third cameras (ii,iii) of this species. The camera occupying the more basal part of the ramification (ii) resulted in an opening to the exterior due to secondary erosion.

Taxonomic description

Spicules: Triactines (Figure 5a–e) are covered by long simple or compound spines arranged in verticils along the rays. Some spicules show reduced spines or are completely smooth (Figure 5d,e). Rays are generally straight, but triactines with one or more curved rays are also common (Figure 5a,e). Some rare forms with four rays are also present (Figure 5f). Ray measurements: 75 (86.3 ± 6.6) 100 × 17.5 (20.9 ± 3.5) 25 μm. Nodular amphiasters have six short rays organised in verticils (Figure 5g,h); spines are organised in knobs at the extremities. The axis is 15 (20 ± 4) 25 μm long and the rays are 2.5 (5 ± 1.4) 7.5 μm. Longer and thinner amphiasters (Figure 5h) have short spines scattered along the rays and are more gathered at the extremities. The axis is 21 (25.3 ± 4) 32.5 μm long, and the short, conical, spiny rays are 7.5 (10 ± 2.8) 12.5 μm. Rare, very small, straight amphiasters with spines concentrated at the extremities and rare spines along the shaft (Figure 5i), about 7.5 μm long.

In the tissue, numerous armed larvae covered with discotriaenes (Figure 5k,l) and slightly curved oxeas (Figure 5j), often with rounded extremities were found (several broken, n = 4, 740–1230 μm). The discotriaenes are flattened and with an irregular quadrangular shape and measure 82.5 (94.6 ± 10.8) 112.5 μm. The outer surface has a depression with a rough surface (Figure 5k), while the inner surface is smooth and convex (Figure 5l).

Erosion pattern: This species eroded mainly the central section of the coral ramification (Figure 4b), excavating three large irregular cavities 2.4–5.1 × 4.1–7.8 mm separated from each other by a relatively short connecting duct of 2.9 ± 0.25 mm in length (Figure

4c,d; File S1; Table S1). From the cavities, some papillary channels, 0.4–0.9 mm long, developed to the coral surface opening in papillae, with diameters ranging from 0.1 to 0.3 mm (Table S1). SEM observation of the chambers provided evidence of the presence of the typical pits with superimposed radial etchings usually produced by the species of the genus *Alectona* (Figure 3b). The diameter of the pits is on average (±SD) 53.3 ± 8.6 μm (Table S1).

Remarks

The spicule set, and in particular the presence of triactines, is unusual for species of this genus, and it has been found exclusively in *Alectona triradiata* (Lévi and Lévi, 1983), described for the Pacific Ocean also boring in the scleraxis of *Pleurocorallium elatius* (Ridley, 1882) [20]. The new species differs from *A. triradiata* in having characteristic nodular amphiasters *Thoosa*-like and in the absence of thin, slender amphiasters, with pointed extremities.

Etymology

It is named after prof. Riccardo Cattaneo-Vietti, who prematurely passed away, in consideration of his research on the Mediterranean red coral.

Genus *Thoosa* Hancock, 1849

Thoosa armata Topsent, 1888

Material

Two small fragments of *C. rubrum* 2.1 × 0.5 cm and 1.5 × 1 cm, respectively (CT5, Figure 6d), were infested by this species.

Taxonomic description

Spicules: Small nodular amphiasters have two verticils of six, spiny knobs (Figure 7a) sometimes with thinner axis and longer rays (Figure 7b); measurements are 10.9 (24.2 ± 7.8) 38.4 × 2.3 (8 ± 4.1) 14.2 μm. Large amphiasters with six, straight, thin, and long rays are arranged in two verticils; spines are grouped at the extremities giving them a knob-like appearance (Figure 7c). Some spines are also scattered along the axis and the rays. Measurements are 40 (49.6 ± 7.2) 59.5 × 2-4 μm. Larger amphiasters, with six, straight, long, and thick rays are arranged in two verticils and end with pointed tips surrounded by small spines (Figure 7d). Measurements are 41.5 (51.5 ± 5.2) 66 × about 14 μm. Oxyasters, biradiate (Figure 7e), sometimes have three- or four- radiated (Figure 7f,g), are wing-like, ending with pointed tips and presenting a central swelling. The rays measure 40 (56.2 ± 9.1) 74 × about 2–3 μm. Ovoid accessory microscleres (Figure 7h); their longer diameter measure 18–28.2 μm (only four measured).

Erosion pattern: T. armata eroded mainly the central section of the coral axis, producing irregular chambers from ellipsoidal to subspherical shapes, with diameters ranging from 1.8 to 3.9 mm, and lengths from 0.6 to 1.8 mm (Figure 6b,e; File S1; Table S1). Cameras were connected by numerous short ducts of 1.3 ± 0.4 mm in length, often found fused together, presenting thicker eight-shaped channels (Figure 6c,f; Table S1). Abundant papillae were observed on micro-CT reconstructions, with a diameter of 0.09–0.2 mm; papillary channels were 0.57–1.58 mm long (Table S1). In the SEM images, the walls of the erosion chambers showed ovoid pits of diameters of 60 ± 9 μm, on average (±SD), and with the surface incised by concentric marks and superimposed radial incisions (Figure 3c; Table S1).

Remarks

T. armata has been described, for the first time, in Gabon (West Africa), and our sample fully agrees with the original description. This species showed erosion scars characterised by circular and radial ornamentations typical of the species of the genus *Alectona*, as already reported in the same samples by Pica et al. [15] and Carballo et al. [16] in *Thoosa* spp. from the Mexican Pacific Ocean.

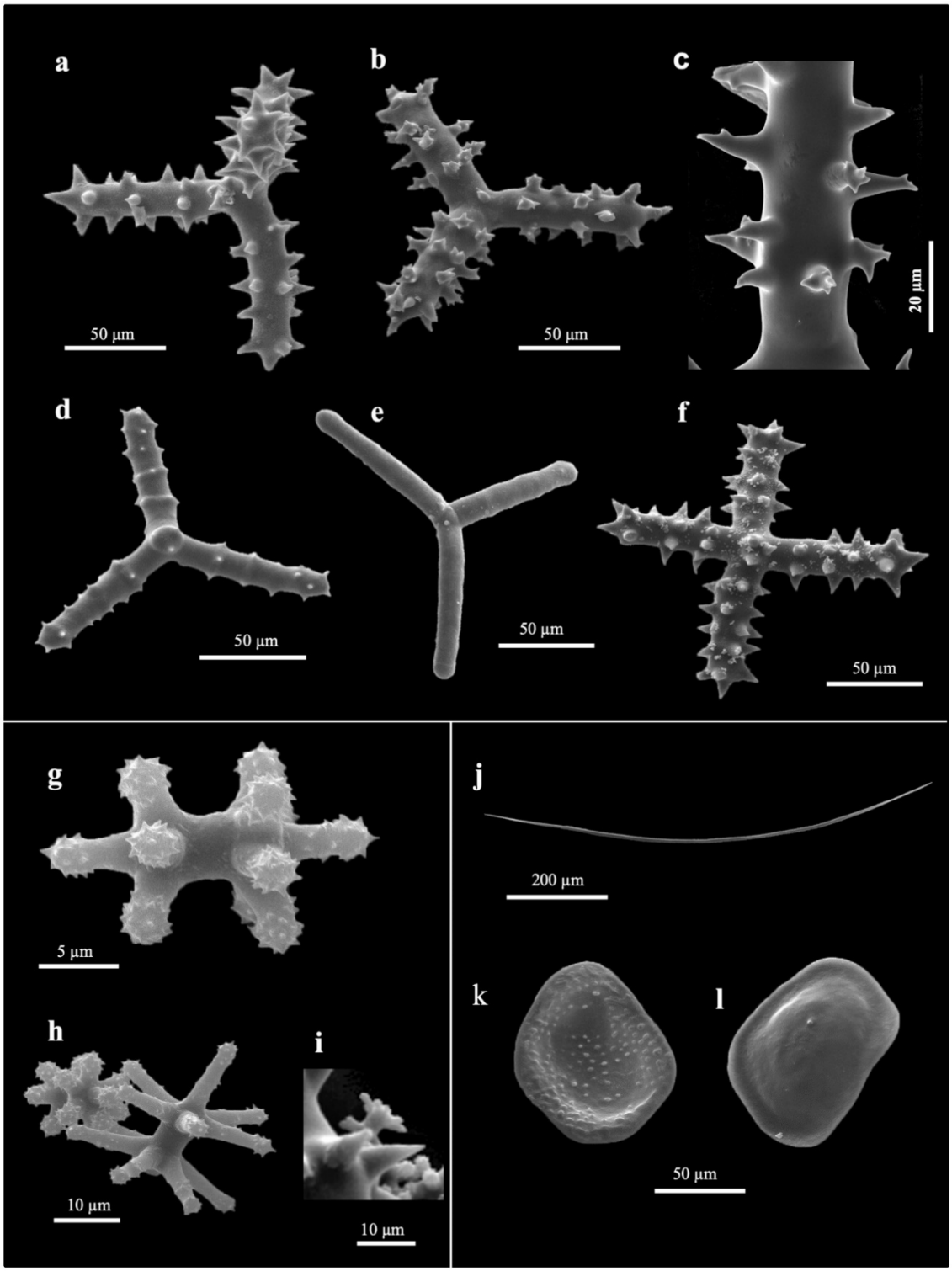

Figure 5. Spicule composition of *Alectona ricardi* sp. nov. present in the red coral sample. SEM images: (**a**,**b**) triactines covered by triangular spines; (**c**) magnification of a ray showing the compound spines; (**d**) slightly spined triactine with spines clearly organised in verticils; (**e**) smooth triactine; (**f**) triactine with four rays; (**g**) nodular amphiaster; (**h**) nodular amphiaster (in the background) and thinner amphiaster; (**i**) very small amphiaster; (**j**) oxea of an armed larva; (**k**) outer surface of a quadrangular discotriaene; (**l**) inner surface of a quadrangular discotriaene.

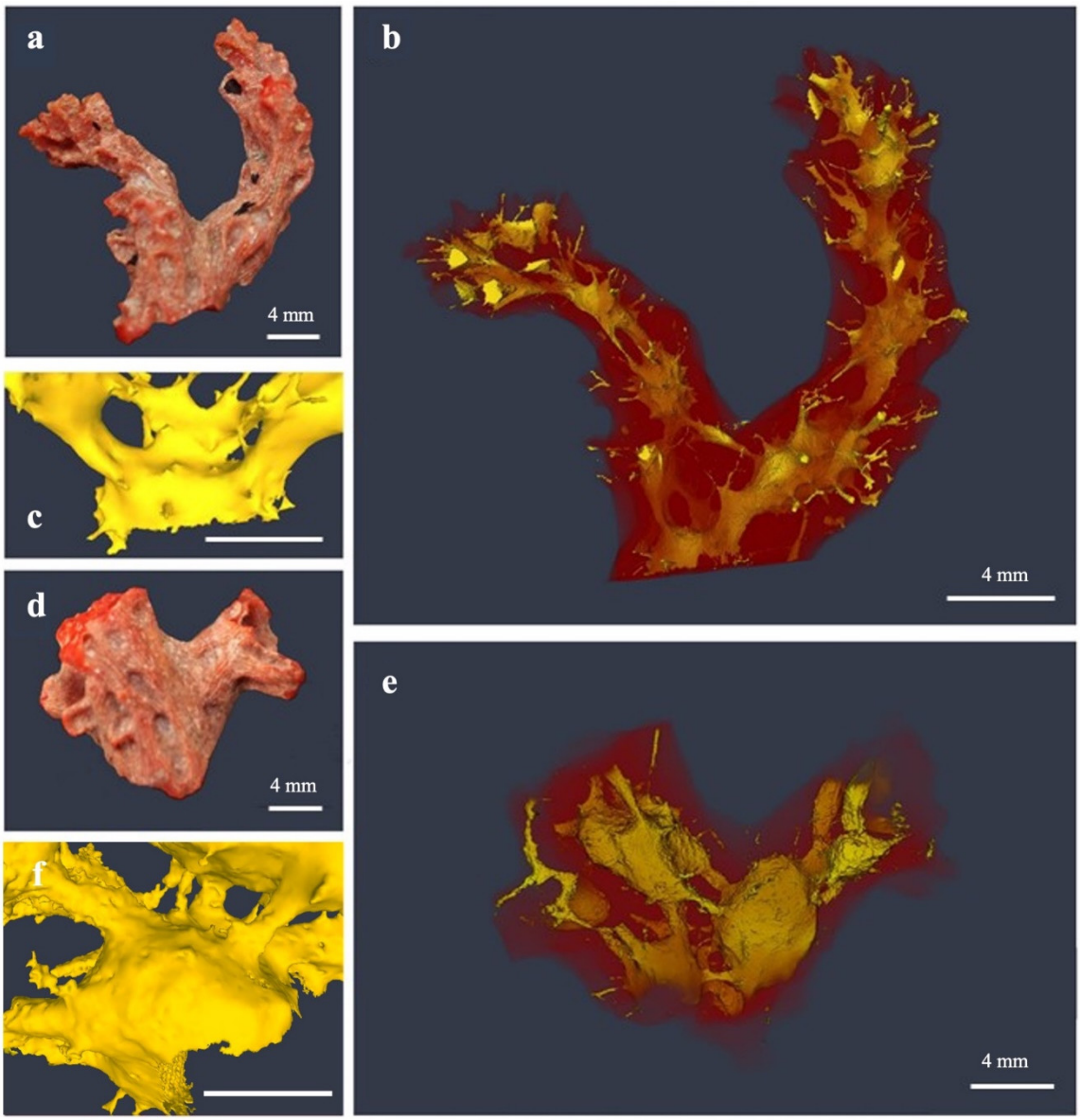

Figure 6. Three-dimensional visualisation of the two red coral samples excavated by *Thoosa armata* from micro-CT reconstructions: (**a**,**d**) red coral samples CT6 and CT5, respectively; (**b**,**e**) eroded cavities represented in yellow and coral in transparent red; (**c**,**f**) details of *T. armata* erosive pattern. Scale bars in (**c**,**f**) equal to 2 mm.

Morphometrics and erosive patterns obtained from *Thoosa* were compared with previously described ichnotaxa, and among these, the trace marker of *Entobia geometrica* (Bromley and d'Alessandro, 1984) resembled those produced by the living species *T. armata*. The traces left by this species fit the typical description of *E. geometrica* [18] in the size and shape of its erosive patterns; additionally, in our samples, it is possible to recognise the growth phases B and C, stages characterised by oval to subspherical shaped chambers (size from 1.0 to 3.7 mm) (Figure 6b,e), connected by two-to-three connecting ducts (Figure 6c,f), frequently fused together (Figure 6c), and presenting numerous pioneer filaments (Figure 6a).

Order Clionaida Morrow and Cárdenas, 2015
Family Clionaidae d'Orbigny, 1851
Genus *Dotona* Carter, 1880
Dotona pulchella mediterranea Rosell and Uriz, 2002
Material

Three different fragments of *C. rubrum* were infested by this species. One fragments (CT2, Figure 8), 1.5 cm high and 0.6 cm in its basal diameter, was exclusively bored by *D. pulchella mediterranea*; a second colony 5.5 cm high with a diameter of 2.5 cm at its base, was also excavated by *A. millari* and *A. ricardi* sp. nov. (CTX, Figures 1d and 4a; File S1). In the third sample (CT3, Figure 1a; File S1), 1.7 cm in height and 0.8 cm in diameter, *A. millari* was also present.

Taxonomic description

Spicules: Microstrongyles with rounded ends and microspined tubercles are spirally arranged. They are often curved or bent especially towards one extremity (Figure 9a–c). They measure 48.8 (63.6 ± 6.8) 72.5 × 5 (6.1 ± 0.7) 7.5 μm, with very thin styles having 95 (108.5 ± 12.3) 117.5 x <2 μm (Figure 9d).

Spiny diplasters measure 12.5 ± 15 μm (only four detected and measured, not illustrated in Figure 9).

Erosion pattern: In all samples, the erosion of *D. pulchella mediterranea* developed mainly in the external part of the coral skeleton, with a moniliform perforation pattern (Figure 8b,e), characterised by numerous chambers organised in strings, and connected by constrictions in advanced erosion phases or long thin connecting ducts in the initial stages; commonly, these intersections present an L-, X-, or T-shape (Figure 8c–f). The species produced chambers measuring 0.6–0.9 × 1.5–9.56 mm (Table S1). Papillae were not observed. SEM analysis showed small pits characterised by concentric incisions, which are more evident towards the peripheral part and less evident in the centre; they have an averaged diameter (±SD) of 31.2 ± 6.5 μm (Table S1).

Remarks

Our specimen fits the description of the subspecies from the Mediterranean [21], differing only in the absence of macroscleres.

From the comparison of the erosive patterns and dimensions with the ichnotaxa described in the literature, we found great similarities between *D. pulchella mediterranea* and *Entobia cateniformis* (Bromley and d'Alessandro, 1984), in which systems were reported as a complex of cylindrically elongated chambers, connected by constrictions and organised in rows with different types of intersections. In the present samples eroded by *D. pulchella mediterranea*, it was possible to identify resemblances within all *E. cateniformis* growth phases (A-D)—from the thin pioneer filaments characteristic of phase A to the network of interweaving chains from phase D, passing through the intermediate phases defined by the development of the cylindrical chains and the creation of the intersections (T, L, X) by anastomosis and dichotomy [16].

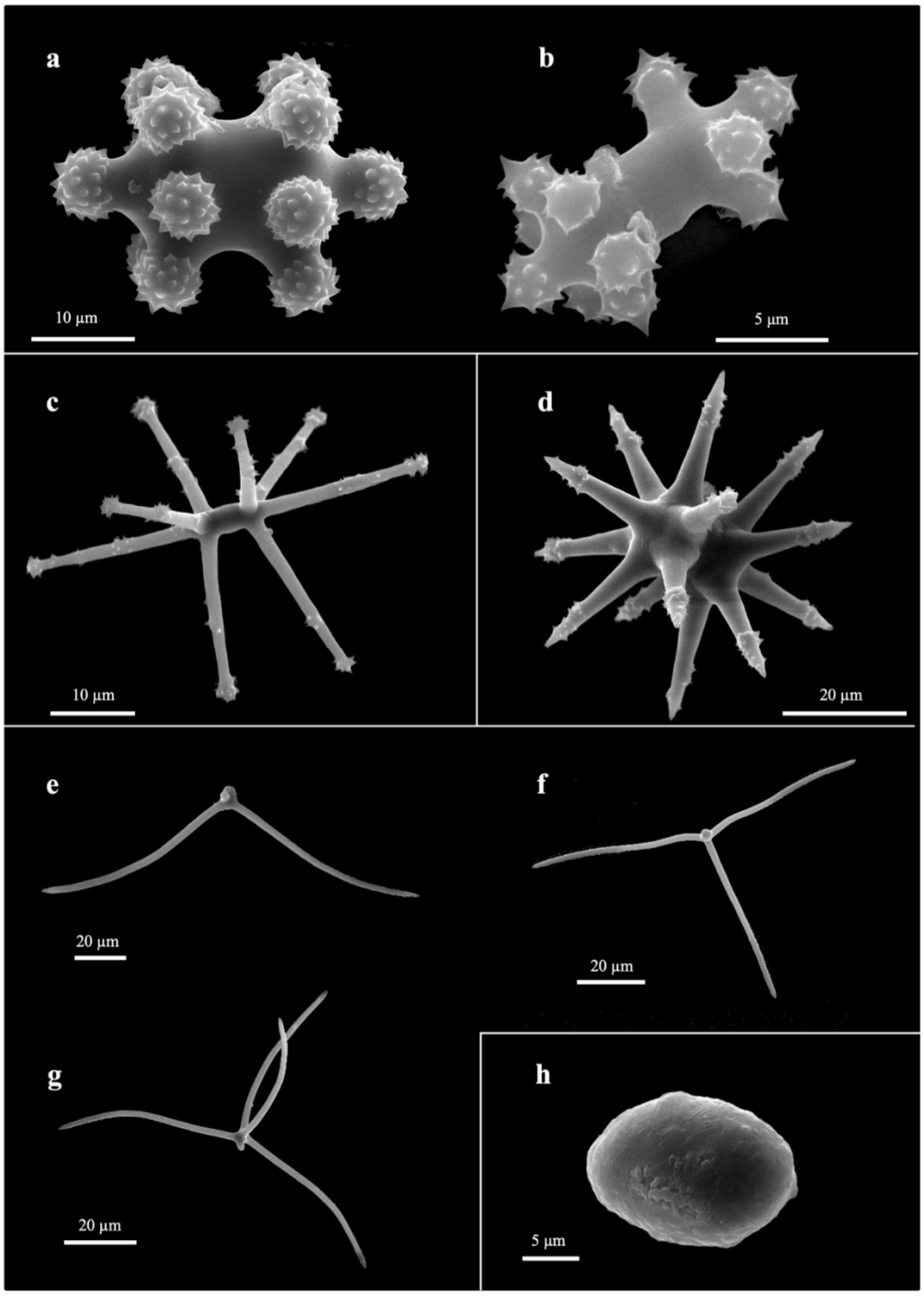

Figure 7. Spicule composition of *Thoosa armata*. SEM images: (**a**) typical nodular amphiaster; (**b**) nodular amphiaster with thinner axis; (**c**) amphiaster with six, straight and long rays arranged in two verticils; (**d**) larger amphiaster with pointed tips surrounded by small spines; (**e**) biradiate oxyaster; (**f**) biradiate oxyaster becoming triradiate; (**g**) oxyaster with four rays; (**h**) ovoid accessory microsclere.

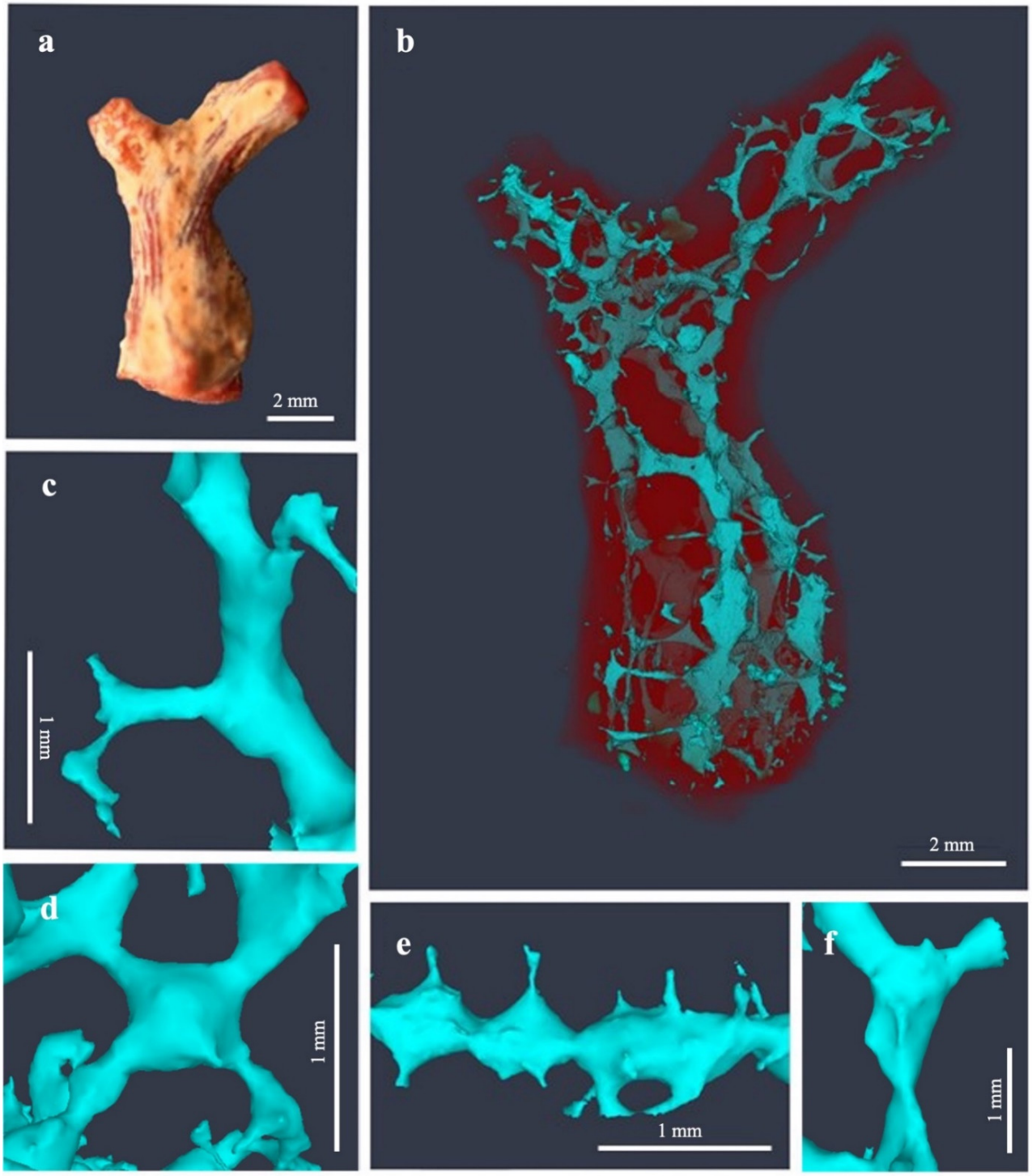

Figure 8. Three-dimensional visualisation of the red coral sample excavated by *Dotona pulchella mediterranea*, from micro-CT reconstructions: (**a**) red coral sample CT2; (**b**) *D. pulchella mediterranea* cavities represented in blue and coral in transparent red; (**c**–**e**) different shape of chamber intersections: L, X, and T-shaped, respectively; (**f**) moniliform perforation pattern produced by *D. pulchella mediterranea*.

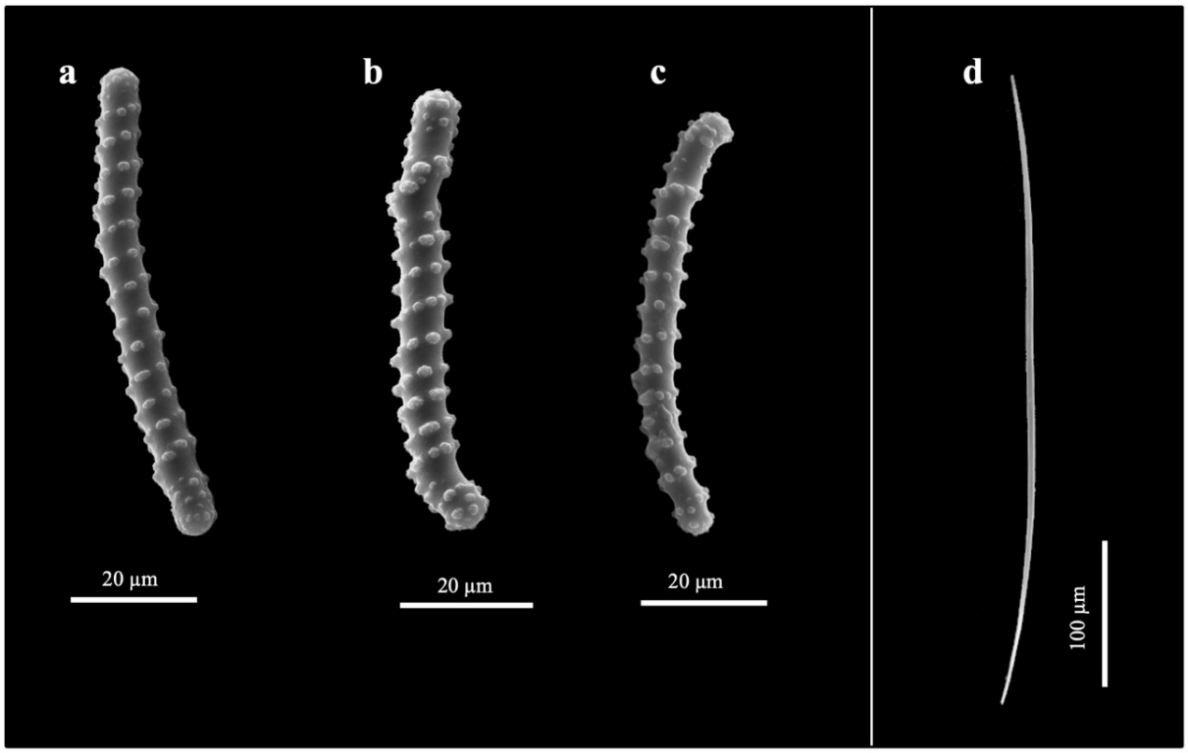

Figure 9. Spicule composition of *Dotona pulchella mediterranea*. SEM images: (**a**–**c**) microstrongyles with microspined tubercles, spirally arranged; (**d**) style.

4. General Remarks

Traditionally, studies on the three-dimensional architecture of sponge bioerosion have been implemented by the application of invasive methods, mainly based on substrate removal [22,23]. Here, for the first time, the bioerosion in the red coral was approached via micro-CT to better understand the development of channels and chambers of the sponge inside the coral scleraxis and to quantify the percentage of the eroded substrate. The erosion activity here evaluated varied in the examined species. *Dotona pulchella mediterranea* removed a lower percentage of coral scleraxis (7.79%) than *Thoosa armata* (20.08% and 13.48%), a sponge usually producing chambers larger than *D. pulchella mediterranea*. Unfortunately, it was not possible to extrapolate the percentage of substrate removed by the single *Alectona* species but to calculate only the total eroded volume, due to the close presence of several species in the same coral sample, producing an intricate boring system. Using micro-CT, Schönberg and Shields [11] evaluated the bioerosion in the spar produced by *Cliona celata* (Grant, 1826) and *Cliona orientalis* (Thiele 1900), two Australian boring species belonging to the same family as *Dotona,* obtaining higher values (up to 48%) of the eroded substrate. The different value of bioerosion is not surprising, considering that it strongly varies in function of the species, the nature of the substrate, its growth phase/age, and the different environmental conditions to which samples were subjected [24]. Moreover, the limited size of the substrate (as is the case of the studied samples), and the presence of several species excavating the same sample, affect the erosion activity of the boring species [16]. In fact, *A. millari* excavated chambers of different sizes and shapes, even inside the same sample (CTX, Figures 1 and 4; Table S1), which is probably a consequence of the competition among the boring sponges for the available substrate. These alternative patterns have been previously defined as stenomorphic boring patterns [16], occurring when a sponge is constricted by physical substrate restrictions [15]. In addition, galleries produced by *A. millari*, *A. ricardi* sp. nov., and *D. pulchella mediterranea* seemed to merge in some areas, even though boring sponges are believed to avoid contact within the same substrate [25]. The observed pattern may be related to the

different moments of colonisation after the primary chambers have remained empty, as it has been already observed for other clionaid species, which colonised and enlarged empty cavities during their development into the substrate [26].

Based on the three-dimensional reconstructions of the sponge chambers' systems and morphometric data extracted from the samples, our results were compared with the descriptions of different *Entobia* species (i.e., sponge bioerosion traces). The change in boring behaviour of some species during their growth, the wide range of factors influencing it, and the similar erosive patterns produced by different species make it difficult to attribute a boring pattern to a single species. Throughout the literature, many *Entobia* have been attributed to different species of clionaids considering the morphological characteristics of the cavities [17]; an example is *Entobia cateniformis*, ichnospecies firstly attributed to *Cliona vermifera* (Hancock, 1867) by Bromley and D'Alessandro [17], while Färber et al. [13] assigned it to *Cliona schmidtii* (Ridley, 1881), and more recently, Turicchia et al. [27] attributed it to *Cliona viridis*. Conversely, our results in this study suggested *E. cateniformis* as a possible trace marker for *D. pulchella mediterranea*.

The analysis and description of endolithic bioerosion patterns have always been challenging tasks. Currently, owing to the application of innovative techniques such as micro-CT, new possibilities arise, allowing researchers to record, from a three-dimensional perspective, the erosive traces present in the substrate. Through this process, a scaled digital cast is obtained, facilitating the storage and sharing of erosive patterns. The development of public repositories to properly store, categorise, and virtually manipulate these casts should be promoted, contributing to the shift from two- to three-dimensional approaches in bioerosion studies. In addition, the creation of labelled three-dimensional database of erosive patterns can be useful for the development of tailored algorithms, which would help in the close future with the semi-automated segmentation of erosive patterns, especially when more than one entity is present in the same sample.

Even though micro-CT represents an innovative tool in the study of boring organisms, it is important to acknowledge its limitations: (1) the need for a powerful scanner to approach very small features (<10 μm) as, for example, papillae channels, sponge spicules, pioneer filaments or chips; and (2) the separation of erosion traces of different sponges when more than one species is present in a sample (as observed in samples CT3 and CTX; Figures 1 and 4). In our case, resolution restrictions were overcome by the coupling of SEM observations to the study, while, by analysing the spicule set present in the traces left behind by sponges, together with the characterisation of the pits eroded in the chamber walls, it was possible to assign the erosive systems to each of the species identified inside the coral scleraxis.

A remarkably high number of species have been recorded so far infesting the red coral scleraxis [28], increasing habitat biodiversity [6,29] but reducing the commercial value of the coral skeletons on the jewellery market [5]. In the following decades, a general increment of the bioeroders' activity is expected, caused by the warming trend, along with the organic pollution affecting coastal areas [30,31]. Despite the apparently low percentage of skeleton removal, the analysed boring sponges may compromise, both the economic value and the coral structural integrity. The impact of boring sponges was already observed in tropical reefs, where they promote scleractinian corals fragmentation [32,33]. Also in temperate habitats, despite their lower bioerosion rates, boring sponges represent the main corals' macroborers, affecting corals' adhesion and persistence on the substrate, likely facilitating their detachment [1,34,35]. In the Mediterranean Sea, where *Corallium rubrum* is endemic and generally grows on coralligenous bioconstruction, it has been documented that the sponge diversity is higher inside respect outside in coralligenous accretions [36]. In this habitat, boring sponges can be considered as intermediate disturbers, shaping coralligenous assemblages' composition and complexity [34], the same action they perform in coral reefs. The three-dimensional structure and the architectural complexity of coralligenous epibenthic assemblages may be considered an effective proxy of coralligenous health status [37], the level of boring sponge infestation of erect calcareous

colonies can clearly affect the long-term stability of this vertical layer. As for tropical reefs, the variability in bioerosion rates and bioeroder abundances severely impacts many reef attributes (i.e., habitat heterogeneity, net reef accretion, and framework integrity) [1]. Therefore, the mapping of the epi- and endolithic organisms can represent a useful tool in the monitoring and definition of coral reefs' ecological status [15].

To conclude, considering all these aspects, together with the general lack of knowledge on the red coral bioerosion, studies such as the one presented in this paper are necessary to better understand the balance between bioconstruction and bioerosion acting in temperate reefs and the many factors affecting these fundamental but neglected processes.

Supplementary Materials: The following is available online at http://www.mdpi.com/, Table S1: Summary of metrics extracted from the eroded traces by micro-CT analysis, File S1: Sponge digital casts obtained from the processing of red coral samples.

Author Contributions: T.P.M. and C.R. contributed to digital cast analysis, data visualisation and curation, description of erosive traces, and writing—reviewing and editing. B.C. contributed to conceptualisation, supervision, project administration, methodology, morphological work, writing–original draft preparation, and writing—review and editing. D.P. and M.B. contributed to morphological work, conceptualisation, and writing—review and editing. G.B. and C.C. contributed to conceptualisation, supervision, and writing—review and editing. All authors have read and agreed to the published version of the manuscript.

Funding: This research received no external funding.

Institutional Review Board Statement: Not applicable.

Informed Consent Statement: Not applicable.

Data Availability Statement: All data produced during this study is available in the Supplementary Material or upon request.

Acknowledgments: The authors would like to thank the Museo Civico di Storia Naturale G. Doria of Genova (Italy) for kindly providing the studied material and Maria Laura Gatto (CISMiN, Università Politecnica delle Marche, Italy) for her assistance during the micro-CT processing.

Conflicts of Interest: The authors declare that they have no conflict of interest.

References

1. Weinstein, D.K.; Maher, R.L.; Correa, A.M.S. Bioerosion. In *Mesophotic Coral Ecosystems. Coral Reefs of the World*; Loya, Y., Puglise, K., Bridge, T., Eds; Springer: Cham, Switzerland, 2015; Volume 12, pp. 829–847. https://doi.org/10.1007/978-3-319-92735-0_43.
2. Calcinai, B.; Cerrano, C.; Bavestrello, G.; Milanese, M.; Sarà, M. Il popolamento di spugne perforatrici di *Corallium rubrum* e di alcuni madreporari del Promontorio di Portofino. *Boll. Mus. Ist. Biol. Univ. Genova* **2002**, *64*, 53–59.
3. Azzini, F.; Calcinai, B.; Iwasaki; N., Bavestrello, G. A new species of *Thoosa* (Demospongiae, Hadromerida) excavating precious coral *Corallium* sp. From Midway. *Ital. J. Zool.* **2007**, *74*, 405–408. https://doi.org/10.1080/11250000701632790.
4. Calcinai, B.; Cerrano, C.; Iwasakei, N.; Bavestrello, G. Sponges boring into precious corals: An overview with description of a new species of *Alectona* (Demospongiae, Alectonidae) and a world-wide identification key for the genus. *Mar. Ecol.* **2008**, *29*, 273–279. https://doi.org/10.1111/j.1439-0485.2008.00246.x.
5. Liverino, B. *Il Corallo: Esperienze e Ricordi di un Corallaro*; Bologna (Italy) Analisi: Bologna, Italy, 1984.
6. Corriero, G.; Abbiati, M.; Santangelo, G. Sponges inhabiting a Mediterranean red coral population. *Mar. Ecol.* **1997**, *18*, 147–155. https://doi.org/10.1111/j.1439-0485.1997.tb00433.x.
7. Rützler, K. Family Clionaidae D'Orbigny, 1851. In *Systema Porifera;* Springer: Boston, MA, USA, 2002; pp. 173–185. https://doi.org/10.1007/978-1-4615-0747-5_19.
8. Vacelet, J. Planktonic armoured propagules of the excavating sponge Alectona (Porifera: Demospongiae) are larvae: Evidence from *Alectona wallichii* and *A. mesatlantica* sp. nov. *Mem. Queensl. Mus.* **1999**, *44*, 627–642.
9. Calcinai, B.; Bavestrello, G.; Cerrano, C. Bioerosion micro-patterns as diagnostic characteristics in boring sponges. *Boll. Mus. Ist. Biol. Univ. Genova.* **2004**, *68*, 229–238.
10. de Voogd, N.J.; Alvarez, B.; Boury-Esnault, N.; Carballo, J.L.; Cárdenas, P.; Díaz, M.-C.; Dohrmann, M.; Downey, R.; Hajdu, E.; Hooper, J.N.A.; et al. World Porifera Database. 2022. Available online: https://www.marinespecies.org/porifera (accessed on 3 February 2022).

11. Schönberg, C.H.; Shields, G. Micro-computed tomography for studies on *Entobia*: Transparent substrate versus modern technology. In *Current Developments in Bioerosion;* Springer: Berlin/Heidelberg, Germany, 2008; pp. 147–164. https://doi.org/10.1007/978-3-540-77598-0_8.
12. Beuck, L.; Vertino, A.; Stepina, E.; Karolczak, M.; Pfannkuche, O. Skeletal response of *Lophelia pertusa* (Scleractinia) to bioeroding sponge infestation visualised with micro-computed tomography. *Facies* **2007**, *53*, 157–176. https://doi.org/10.1007/s10347-006-0094-9.
13. Färber, C.; Titschack, J.; Schönberg, C.H.L.; Ehrig, K.; Boos, K.; Baum, D.; Wisshak, M. Long-term macrobioerosion in the Mediterranean sea assessed by micro-computed tomography. *Biogeosciences* **2016**, *13*, 3461–3474. https://doi.org/10.5194/bg-13-3461-2016.
14. Rützler, K. The burrowing sponges of Bermuda. *Smithson. Cont. Zool.* **1974**, *165*, 32. https://doi.org/10.5479/si.00810282.165.
15. Pica, D.; Calcinai, B.; Bertolino, M. Excavating sponges boring into the precious red coral from Cape Verde Archipelago. *Biol. Mar. Mediterr.* **2011**, *18*, 278–279.
16. Carballo, J.L.; Bautista-Guerrero, E.; Cárdenas, P.; Cruz-Barraza, J.A.; Aguilar-Camacho, J.M. Molecular and morphological data from Thoosidae in favour of the creation of a new suborder of Tetractinellida. *Syst. Biodivers.* **2018**, *16*, 512–521. https://doi.org/10.1080/14772000.2018.1457100.
17. Beuck, L.; Freiwald, A. Bioerosion patterns in a deep-water *Lophelia pertusa* (Scleractinia) thicket (Propeller Mound, northern Porcupine Seabight). In *Cold-Water Corals and Ecosystems*; Springer: Berlin/Heidelberg, Germany, **2005**; pp. 915–936. https://doi.org/10.1007/3-540-27673-4_47.
18. Bromley, R.G.; D'Alessandro, A. The ichnogenus *Entobia* from the Miocene, Pliocene and Pleistocene of southern Italy. *Riv. Ital. Paleontol. Stratigr.* **1984**, *90*, 227–296.
19. Bromley, R.G.; D'Alessandro, A. Ichnological study of shallow marine endolithic sponges from the Italian coast. *Riv. Ital. Paleontol. Stratigr.* **1989**, *95*, 279–314.
20. Bavestrello, G.; Calcinai, B.; Cerrano, C.; Sara, M. *Alectona* species from North-Western Pacific (Demospongiae: Clionidae). *J. Mar. Biol. Ass. UK* **1998**, *78*, 59–73. https://doi.org/10.1017/S0025315400039965.
21. Rosell, D.; Uriz, M.J. Excavating and endolithic sponge species (Porifera) from the Mediterranean: Species descriptions and identification key. *Org. Divers. Evol*. **2002**, *2*, 55–86. https://doi.org/10.5194/bg-2015-653.
22. Golubić, S.; Friedmann, I.; Schneider, J. The lithobiontic ecological niche, with special reference to microorganisms. *J. Sediment. Res.* **1981**, *51*, 475–478. https://doi.org/10.1306/212f7cb6-2b24-11d7-8648000102c1865d.
23. Wisshak, M.; Knaust, D.; Bromley, R.G. (Eds.) *Trace Fossils as Indicators of Sedimentary Environments, Developments in Sedimentology*; Elsevier: Amsterdam, The Netherlands, 2012; Volume 64, pp. 213–243. https://doi.org/10.1016/B978-0-444-53813-0.00008-3.
24. Davidson, T.M.; Altieri, A.H.; Ruiz, G.M.; Torchin, M.E. Bioerosion in a changing world: A conceptual framework. *Ecol. Lett.* **2018**, *21*, 422–438. https://doi.org/10.1111/ele.12899.
25. Bromley, R.G.; Tendal, O.S. Example of substrate competition and phobotropism between two clionid sponges. *J. Zool.* **1973**, *169*, 151–155.
26. Hoeksema, B.W. Excavation Patterns and Spiculae Dimensions of the Boring Sponge *Cliona celata* from the SW Netherlands. *Senckenb. Marit*. **1982**, *15*, 55–85.
27. Turicchia, E.; Abbiati, M.; Bettuzzi, M.; Calcinai, B.; Morigi, M.P.; Summers, A.P.; Ponti, M. Bioconstruction and Bioerosion in the Northern Adriatic Coralligenous Reefs Quantified by X-Ray Computed Tomography. *Front. Mar. Sci.* **2022**, *8*. https://doi.org/10.3389/fmars.2021.790869.
28. Calcinai, B.; Bavestrello, G.; Cerrano, C.; Sarà, M. Boring sponges living into precious corals from the Pacific Ocean. *Ital. J. Zool.* **2001**, *68*, 153–160. https://doi.org/10.1080/11250000109356400.
29. Bavestrello, G.; Calcinai, B.; Sarà, M. Two new species of *Cliona* (Porifera, Demospongiae) boring the scleraxis of *Corallium elatius* from the western Pacific. *Ital. J. Zool.* **1995**, *62*, 375–381. https://doi.org/10.1080/11250009509356092.
30. Webb, A.E.; van Heuven, S.M.; de Bakker, D.M.; van Duyl, F.C.; Reichart, G.J.; de Nooijer, L.J. Combined effects of experimental acidification and eutrophication on reef sponge bioerosion rates. *Front. Mar. Sci.* **2017**, *4*, 311. https://doi.org/10.3389/fmars.2017.00311.
31. Fang, J.K.; Mello-Athayde, M.A.; Schönberg, C.H.; Kline, D.I.; Hoegh-Guldberg, O.; Dove, S. Sponge biomass and bioerosion rates increase under ocean warming and acidification. *Glob Chang. Biol.* **2013**, *19*, 3581–3591. https://doi.org/10.1111/gcb.12334.
32. Tunnicliffe, V. Breakage and propagation of the stony coral *Acropora cervicornis*. *Proc. Nad. Acad. Sci. USA* **1981**, *78*, 2427–2431. https://doi.org/10.1073/pnas.78.4.2427.
33. Highsmith, R.C. Reproduction by fragmentation in corals. *Mar. Ecol. Prog. Ser.* **1982**, *7*, 207–226. https://doi.org/10.3354/meps007207.
34. Cerrano, C.; Bavestrello, G.; Bianchi, C.N.; Calcinai, B.; Cattaneo-Vietti, R.; Morri, C.; Sarà, M. The role of sponge bioerosion in Mediterranean coralligenous accretion. In *Mediterranean Ecosystems*; Faranda, F.M., Guglielmo, L., Spezie, G.C., Eds.; Springer: Milano, Italy, 2001; pp. 235–240. https://doi.org/10.1007/978-88-470-2105-1_30.
35. Grace, S. Winter quiescence, growth rate, and the release from competition in the temperate scleractinian coral *Astrangia poculata* (Ellis & Solander 1786). *Northeastern Nat.* **2017**, *24*, B119–B134. https://doi.org/10.1656/045.024.s715.

36. Calcinai, B.; Bertolino, M.; Bavestrello, G.; Montori, S.; Mori, M.; Pica, D.; Valisano, L.; Cerrano, C. Comparison between the sponge fauna living outside and inside the coralligenous bioconstruction. A quantitative approach. *Mediterr. Mar. Sci.* **2015**, *16*, 413–418.
37. Valisano, L.; Palma, M.; Pantaleo, U.; Calcinai, B.; Cerrano, C. Characterization of North–Western Mediterranean coralligenous assemblages by video surveys and evaluation of their structural complexity. *Mar. Pollut. Bull.* **2019**, *148*, 134–148.